Magnetic and electrical transport properties of electrodeposited Ni-Cu alloys and $Ni_{81}Cu_{19}/Cu$ multilayers

1999 J. Phys.: Condens. Matter 11 963

(http://iopscience.iop.org/0953-8984/11/4/004)

J. Phys.: Condens. Matter **11** (1999) 963–973. Printed in the UK PII: S0953-8984(99)97906-7

Magnetic and electrical transport properties of electrodeposited Ni–Cu alloys and $Ni_{81}Cu_{19}$/Cu multilayers

I Bakonyi†, E Tóth-Kádár, J Tóth, T Becsei, T Tarnóczi and P Kamasa

Research Institute for Solid State Physics and Optics, Hungarian Academy of Sciences, H-1525 Budapest, POB 49, Hungary

Received 29 September 1998

Abstract. Electrodeposited Ni–Cu alloys and nanoscale Ni–Cu/Cu multilayers were produced by direct-current plating and pulse-plating, respectively. The room-temperature electrical resistivity and thermopower as well as the Curie temperature for the Ni–Cu electrodeposits were in good agreement with relevant data reported for metallurgically processed Ni–Cu alloys. The same parameters were investigated also for the $Ni_{81}Cu_{19}$/Cu multilayers as a function of the constituent magnetic and non-magnetic layer thicknesses. The electrical resistivity of the multilayers was much larger than calculated for a parallel resistance model and their thermopower was more negative than expected on the basis of a volume average model, by using bulk values of both parameters for the sublayer materials. These differences were ascribed to surface scattering processes which can be significant in nanoscale multilayer structures.

1. Introduction

It has been well demonstrated that electrodeposition is an efficient and relatively simple technique to produce metallic multilayers [1] with attractive physical properties. In particular, electrodeposited multilayers such as, e.g. Ni–Cu/Cu, Co–Cu/Cu and Ni–Co–Cu/Cu were also shown to exhibit giant magnetoresistance (GMR) and this topic has been recently summarized by Schwarzacher and Lashmore [2]. Although in comparison with the Co-Cu and Ni–Co–Cu multilayers the magnitude of GMR in the Ni–Cu/Cu system is not very high, a systematic variation of GMR with the individual layer thicknesses could still be observed [3–7].

In order to have a better understanding of the magnetoresistance properties, we have performed a detailed investigation of the variation of the room-temperature electrical resistivity and thermopower with both magnetic and non-magnetic layer thicknesses for electrodeposited $Ni_{81}Cu_{19}$/Cu multilayers. Besides the multilayers, bulk Ni–Cu alloys were also produced by electrodeposition and we determined their resistivity and thermopower as well. The results of these measurements of the electrical transport properties in zero magnetic field will be described in the present paper. As part of the sample characterization, the Curie temperatures were also measured for some of the Ni–Cu alloy and $Ni_{81}Cu_{19}$/Cu multilayer samples. A detailed structural study performed by transmission electron microscopy (TEM) and x-ray diffraction (XRD) has been reported separately [6, 8] whereas the magnetoresistance characteristics will be presented elsewhere [9].

† Corresponding author. E-mail address: bakonyi@power.szfki.kfki.hu.

0953-8984/99/040963+11$19.50

2. Experimental details

Bulk Ni–Cu alloy foils of typically a few micrometres thickness were produced by direct-current (d.c.) plating from a sulphate type bath and the alloy composition was varied by changing the deposition current density (i_{dep}). For $i_{dep} = 2$ mA cm^{-2}, pure Cu deposits were obtained whereas for deposition current densities from 20 to 50 mA cm^{-2}, the alloy composition was about $Ni_{81}Cu_{19}$. For producing the multilayers, we applied the usual single-bath pulse-plating technique in the galvanostatic (current-controlled) deposition mode. We used $i_{dep} = 2$ mA cm^{-2} for depositing the non-magnetic Cu layers and $i_{dep} = 20$ mA cm^{-2} for depositing the magnetic $Ni_{81}Cu_{19}$ layers. The thicknesses of the individual layers were controlled by the length of the deposition current pulses. Bilayer repeat numbers as high as 500 to 5000 were applied so that the total thickness of the multilayer deposits was typically 5 μm. Both the bulk alloy and the multilayer samples were removed from their polycrystalline Ti or Cu foil substrates for the purposes of further studies. More details of the sample preparation process have been described elsewhere [6, 9].

The Curie temperature (T_C) was determined by measuring the magnetization in a magnetic field of $H = 30$ Oe in a Faraday type magnetic balance and/or by measuring the a.c. susceptibility with a home-built a.c. susceptometer.

The in-plane electrical resistivity (ρ) and the thermopower (S) were determined in zero magnetic field at room temperature in the same manner as described recently for electrodeposited nanocrystalline Ni foils [10, 11]. The resistivity was measured by using a conventional four-point d.c. probe and the thermopower data were obtained with the help of a local thermopower probe [12, 13].

3. Results and discussion

3.1. Curie temperature

3.1.1. Bulk Ni–Cu alloys. Figure 1 demonstrates that the T_C values of the electrodeposited Ni–Cu alloys agree well with corresponding data on metallurgically produced samples [14, 15]. The slightly higher T_C values of the electrodeposited alloys may partly come from the presence of about 1 at.% Co impurity in these deposits [9]. Although the temperature range of the magnetic phase transition was fairly large when measured either in the magnetic balance or via the a.c. susceptibility, both measurement techniques yielded essentially the same T_C values (figure 1).

3.1.2. $Ni_{81}Cu_{19}$/Cu multilayers. The Curie points measured for a multilayer series with $d_{Cu} = 0.7$ nm in a magnetic balance are shown in figure 2. As expected, for sufficiently thick Ni–Cu magnetic layers, T_C is as high as the Curie point of the d.c.-plated (bulk) Ni–Cu alloy of the same composition (440 K) whereas T_C decreases with decreasing d_{Ni-Cu}. Qualitatively, this behaviour is similar to that observed for sputtered Ni/Ag multilayers [16]. However, whereas T_C reached practically 0 K at $d_{Ni} = 0.2$ nm and was around 200 K at $d_{Ni} = 0.6$ nm for $d_{Ag} = 1.1$ nm and 1.8 nm [16] in the sputtered Ni/Ag multilayers, the electrodeposited $Ni_{81}Cu_{19}$/Cu multilayers have a Curie point definitely above 300 K even at $d_{Ni-Cu} = 0.6$ nm for $d_{Cu} = 0.7$ nm (figure 2). Such a difference can be explained by the thinner non-magnetic spacer layer in the $Ni_{81}Cu_{19}$/Cu multilayers, enabling a stronger coupling between the constituent magnetic layers. This increased coupling may be either due to an enhanced indirect coupling via conduction electron polarization in the thinner Cu layers or due to a direct coupling of the ferromagnetic layers through the pinholes of the 0.7 nm thick non-magnetic Cu spacer

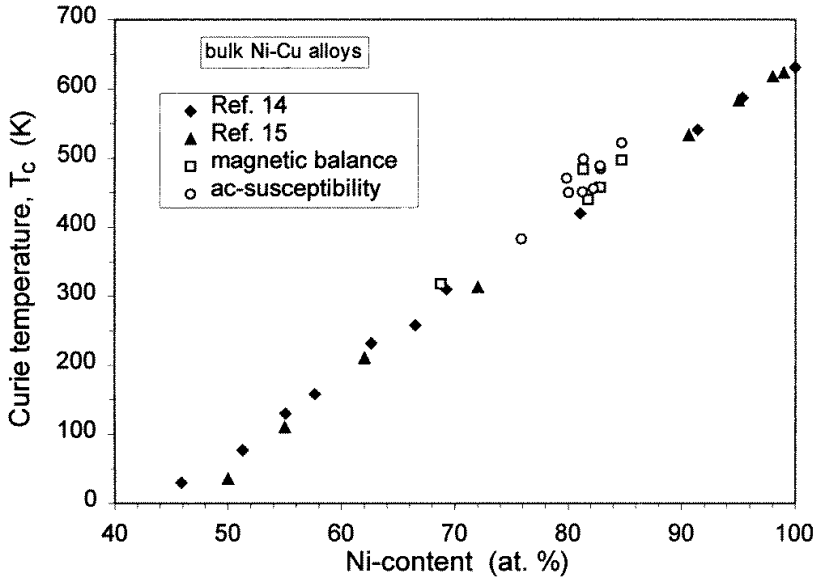

Figure 1. Composition dependence of the Curie temperature (T_C) of metallurgically processed (solid symbols [14, 15]) and electrodeposited (open symbols, this work) bulk Ni–Cu alloys. The electrodeposited alloys may contain about 1 at.% Co [9].

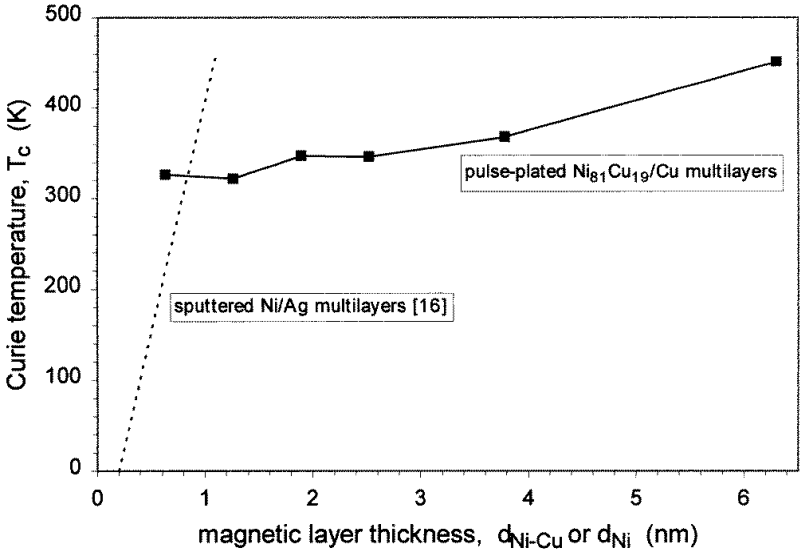

Figure 2. Curie temperature (T_C) of electrodeposited (solid symbols, this work) $Ni_{81}Cu_{19}$/Cu (0.7 nm) multilayers as a function of the Ni–Cu layer thickness (d_{Ni-Cu}). The Curie temperatures of bulk electrodeposited $Ni_{81}Cu_{19}$ alloy and bulk fcc Ni are 440 K (figure 1) and 631 K [14], respectively. The solid line serves as a guide for the eye only. The dashed line gives the T_C data for sputtered Ni/Ag multilayers [16] with $d_{Ag} = 1.1$ nm and 1.7 nm as a function of the Ni layer thickness (d_{Ni}).

layer that may already be discontinuous at such small thicknesses. However, the resistivity measurements performed either in zero magnetic field (section 3.2.2) or in a magnetic field

[9] rather indicate that the Cu spacer layer is continuous at the thickness $d_{Cu} = 0.7$ nm. Furthermore, the zero-field resistivity data (section 3.2.2) suggest that the $Ni_{81}Cu_{19}$ magnetic layer becomes discontinuous below about 1 nm thickness. In view of this latter fact, the observed strength of the coupling between the 'discontinuous' $Ni_{81}Cu_{19}$ layers as evidenced by the Curie point measurements is even more surprising. Anyway, the magnetoresistance behaviour [9] of the sample with $d_{Ni-Cu} = 1.3$ nm and $d_{Cu} = 0.7$ nm also unambiguously indicated the existence of ferromagnetism in this multilayer at room temperature.

3.2. Electrical transport properties in zero magnetic field

3.2.1. Bulk Ni–Cu alloys. For d.c.-plated Cu deposited with $i_{dep} = 2$ mA cm^{-2}, the value of the room-temperature resistivity is about 2 $\mu\Omega$ cm which is very close to the value for pure Cu ($\rho = 1.75$ $\mu\Omega$ cm [17]), with the difference being mostly explainable with the uncertainty of the thickness determination whereas the thermopower agreed within the error of reproducibility (± 0.05 μV K^{-1}) with the pure Cu value (S(Cu) = +2.17 μV K^{-1} [18]). Similarly to the Ni content, both ρ and S remained constant for $i_{dep} \geqslant 20$ mA cm^{-2}. The room-temperature resistivity and thermopower value of the d.c.-plated $Ni_{81}Cu_{19}$ alloy are 34 $\mu\Omega$ cm and -32 μV K^{-1}, respectively, which represent an average obtained on seven independent samples prepared under nominally identical conditions.

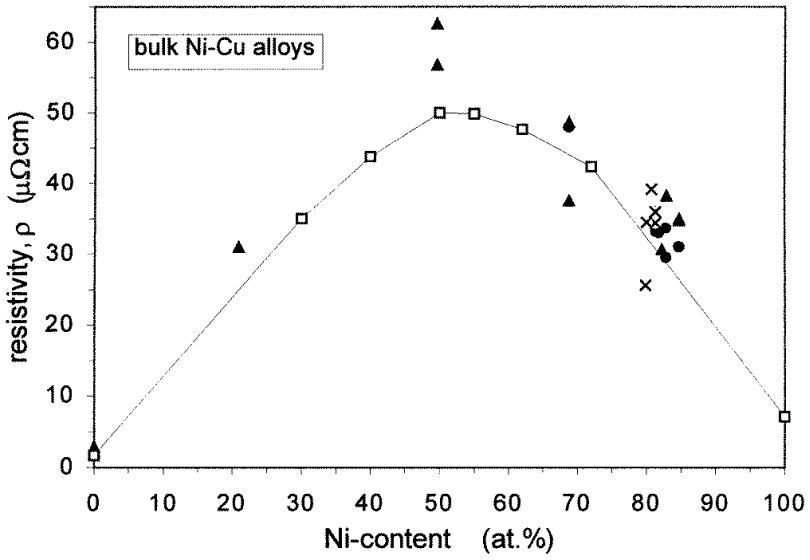

Figure 3. Composition dependence of the room-temperature electrical resistivity (ρ) of metallurgically processed (open square symbols [15]) and electrodeposited (solid symbols and $\times$, this work) bulk Ni–Cu alloys. The different symbols for the electrodeposited alloys refer to different sample series and substrates (Ti or Cu). The solid line serves as a guide for the eye only.

The composition dependence of ρ and S for bulk Ni–Cu alloys is shown in figures 3 and 4, respectively. The general behaviour of the composition dependence of ρ and S for the electrodeposited Ni–Cu alloys is very similar to the results on the metallurgically processed alloys [15] although there are some slight differences. The resistivity data for electrodeposited Ni–Cu appear to be systematically higher, which might indicate a chemically more disordered state in comparison with the metallurgically processed Ni–Cu alloys. Since

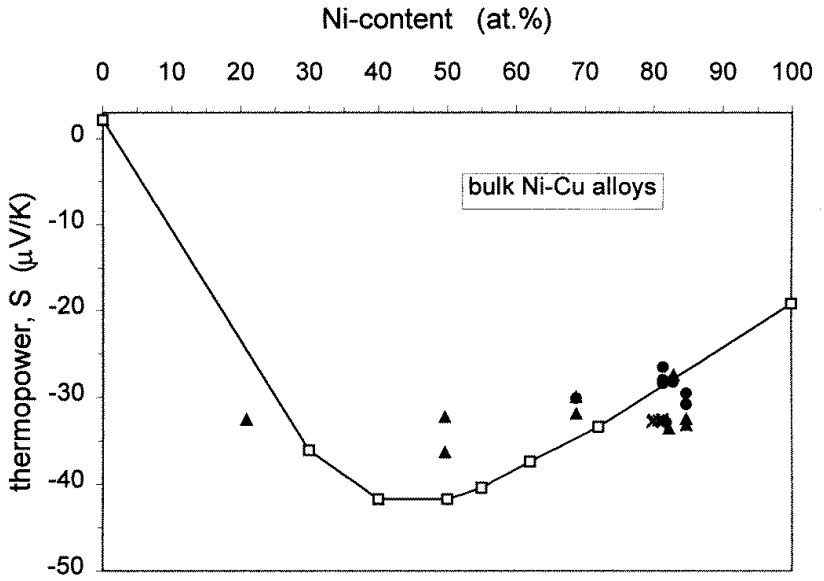

Figure 4. Composition dependence of the room-temperature thermopower (S) of metallurgically processed (open square symbols [15]) and electrodeposited (solid symbols and ×, this work) bulk Ni–Cu alloys. The different symbols for the electrodeposited alloys refer to different sample series and substrates (Ti or Cu). The solid line serves as a guide for the eye only.

electrodeposition is known to result usually in a grain refinement, a smaller crystalline grain size of the electrodeposited Ni–Cu alloys may also contribute to the their higher resistivity as was observed also for electrodeposited Ni [10, 11, 19]. On the other hand, S seems to vary in a more flattened way for the electrodeposited Ni–Cu alloys in the middle of the composition range, the interpretation of which is, however, not so straightforward as in the case of resistivity.

3.2.2. $Ni_{81}Cu_{19}$/Cu multilayers. The room-temperature electrical resistivity of electrodeposited $Ni_{81}Cu_{19}$/Cu multilayers is shown in figure 5 as a function of d_{Ni-Cu}. The two independent series with $d_{Cu} = 0.7$ nm yielded quite well-reproduced results. The ρ values are smaller for $d_{Cu} = 1.4$ nm than for $d_{Cu} = 0.7$ nm and this corresponds to expectation. The sharp drop of ρ for low d_{Ni-Cu} values indicates that at such small thicknesses, the magnetic $Ni_{81}Cu_{19}$ layer is no longer continuous and the $Ni_{81}Cu_{19}$/Cu deposit consists of finely dispersed small islands of the magnetic Ni–Cu component which are embedded in the Cu matrix. At about $d_{Ni-Cu} \approx 1$ nm, the high observed ρ values indicate that the magnetic layer is probably already continuous and there is no direct contact between the Cu layers through pin-holes in the $Ni_{81}Cu_{19}$ layers.

It is remarkable that the resistivity of the $Ni_{81}Cu_{19}$/Cu multilayer is as high as (for $d_{Cu} = 1.4$ nm) or even higher (for $d_{Cu} = 0.7$ nm) than the resistivity ($\rho \approx 34\ \mu\Omega$ cm) of the bulk $Ni_{81}Cu_{19}$ alloy produced by d.c. plating. This means that inserting nanometre-scale Cu layers into an $Ni_{81}Cu_{19}$ alloy did not result in a decrease of the resistivity although for d_{Ni-Cu} values comparable to d_{Cu} ($\approx$1 nm), a considerable fraction of the multilayer structure is pure Cu metal with $\rho \approx 2\ \mu\Omega$ cm.

The reason for this behaviour is due to the multilayered structure consisting of layers with different compositions and with thicknesses in the nanometre range where surface scattering

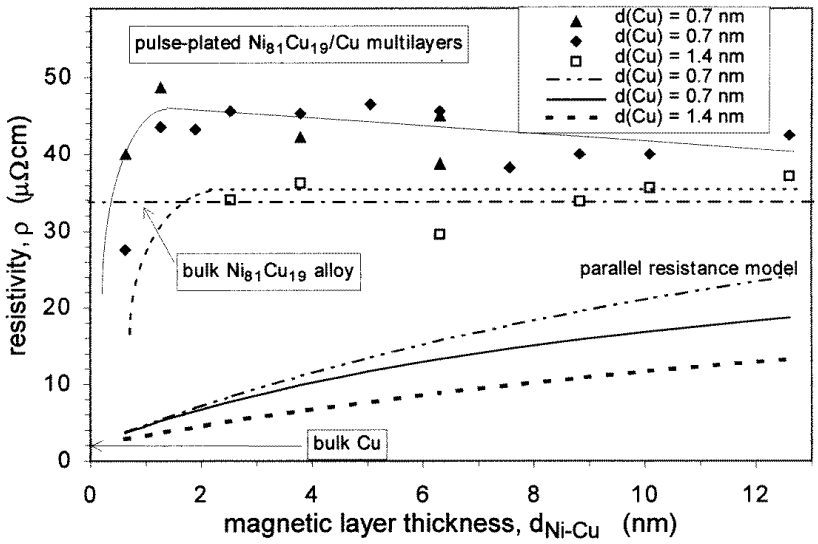

Figure 5. Room-temperature in-plane electrical resistivity (ρ) of electrodeposited $Ni_{81}Cu_{19}$/Cu multilayers with $d_{Cu} = 0.7$ nm (solid symbols, two different series) and 1.4 nm (open symbols) as a function of the Ni–Cu layer thickness (d_{Ni-Cu}). The thin solid and dashed lines through the data points serve as a guide for the eye only. The horizontal dash–dotted line indicates the resistivity of the bulk electrodeposited $Ni_{81}Cu_{19}$ alloy and the arrow to the ρ axis points to the pure Cu resistivity value. The results calculated on the basis of a parallel resistance model by using bulk resistivity values of Cu (2 $\mu\Omega$ cm) and $Ni_{81}Cu_{19}$ (34 $\mu\Omega$ cm) are given by the thick solid ($d_{Cu} = 0.7$ nm) and thick dashed ($d_{Cu} = 1.4$ nm) lines. The double-dot–dashed line gives the calculated resistivity in the above model for $d_{Cu} = 0.7$ nm by assuming that the magnetic layer has a composition of $Ni_{50}Cu_{50}$ exhibiting the maximum resistivity (60 $\mu\Omega$ cm) in the Ni–Cu system (see figure 3).

processes already play an important role in determining the electrical transport properties [20]. This can be further exemplified by the following considerations.

A multilayered structure can be considered as consisting of an N-times repeated sequence of the bilayer composed of layer 1 and layer 2 represented by R_1 and R_2 as resistances in parallel for layer 1 and 2, respectively. Then, the in-plane resistance of the multilayer structure is

$$R = \frac{1}{N}\frac{R_1 R_2}{R_1 + R_2}. \tag{1}$$

On the other hand, it is easy to show that the in-plane resistivity ρ of the multilayer is independent of N and depends on the resistivity and thickness of the constituent layers only (ρ_1 and d_1 as well as ρ_2 and d_2) and is given by the expression

$$\frac{\rho}{d_1 + d_2} = \frac{(\rho_1/d_1)\rho_2/d_2}{\rho_1/d_1 + \rho_2/d_2}. \tag{2}$$

By using $\rho_{Ni-Cu} = 34$ $\mu\Omega$ cm and $\rho_{Cu} = 2$ $\mu\Omega$ cm, we plotted in figure 5 the multilayer resistivity ρ as calculated from equation (2) for $d_{Cu} = 0.7$ nm (thick solid line) and $d_{Cu} = 1.4$ nm (thick dashed line) as a function of d_{Ni-Cu}. As expected, ρ is higher for the smaller Cu layer thickness and increases with an increase of the thickness of the magnetic layer exhibiting a higher bulk resistivity than the non-magnetic layer material. However, these calculated ρ values are well below the experimental data obtained for the corresponding multilayers.

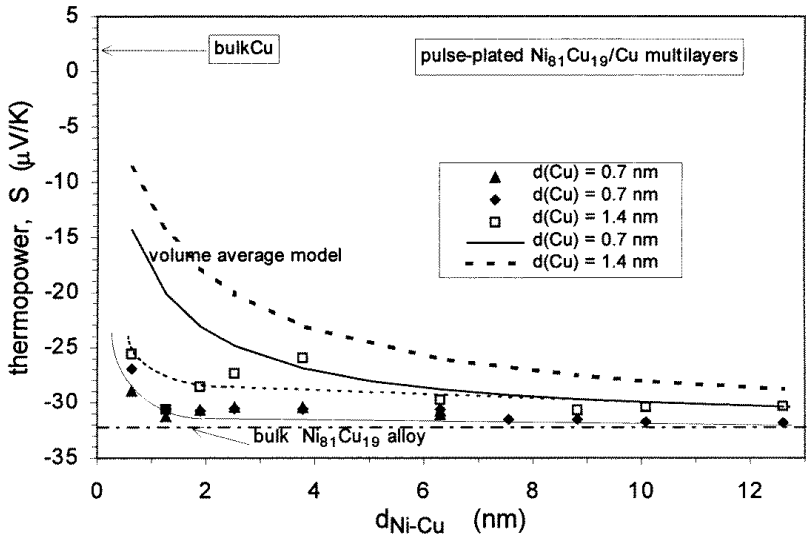

Figure 6. Room-temperature in-plane thermopower (S) of electrodeposited $Ni_{81}Cu_{19}$/Cu multilayers with $d_{Cu} = 0.7$ nm (solid symbols, two different series) and 1.4 nm (open symbols) as a function of the Ni–Cu layer thickness (d_{Ni-Cu}). The thin solid and dashed lines through the data points serve as a guide for the eye only. The horizontal dash–dotted line indicates the thermopower of the bulk electrodeposited $Ni_{81}Cu_{19}$ alloy and the arrow to the S axis points to the pure Cu thermopower value. The results calculated on the basis of a volume average model by using bulk thermopower values of Cu (2.17 μV K^{-1}) and $Ni_{81}Cu_{19}$ (-32 μV K^{-1}) are given by the thick solid ($d_{Cu} = 0.7$ nm) and thick dashed ($d_{Cu} = 1.4$ nm) lines.

In an attempt to explain the observed large multilayer resistivity, we might need to consider also the contribution of the magnetic/non-magnetic interfaces. Namely, due to the pulse-plating deposition technique, we cannot exclude the formation of a thin interface layer between the Cu and $Ni_{81}Cu_{19}$ layers which has an Ni content varying between 0 and 81 at.%. Evidence for this has, indeed, been found also from magnetic and magnetoresistance data [7]. This implies, with reference to figure 3, that this interface layer has a higher resistivity than the $Ni_{81}Cu_{19}$ alloy layer. But even if we assume that the whole of the Ni–Cu magnetic layers consist of an alloy $Ni_{50}Cu_{50}$ for which the resistivity is maximum in the Ni–Cu system with $\rho \approx 60$ $\mu\Omega$ cm (see figure 3), the parallel resistance model of equation (2) leads to only a slight increase of the calculated multilayer resistivity value (double-dot–dash line in figure 5).

Furthermore, since the magnetoresistance of these multilayers is at most 3% [5–7, 9], the contribution of the GMR effect to the resistivity is much smaller than the observed difference between the measured multilayer resistivity and the value calculated in the parallel resistance model.

The dependence of the room-temperature thermopower S on layer thicknesses is shown in figure 6 for the same three sample series. The general behaviour of S is very similar to that of the resistivity, both concerning the thickness dependences and the comparisons to pure Cu and the bulk $Ni_{81}Cu_{19}$ alloy. If we perform a simple volume averaging for the thermopower, we may write the thermopower of the multilayer structure as

$$S = \frac{d_1}{d_1 + d_2} S_1 + \frac{d_2}{d_1 + d_2} S_2 \tag{3}$$

where S_1 and S_2 are the thermopowers of layer 1 and 2, respectively. These calculated S values

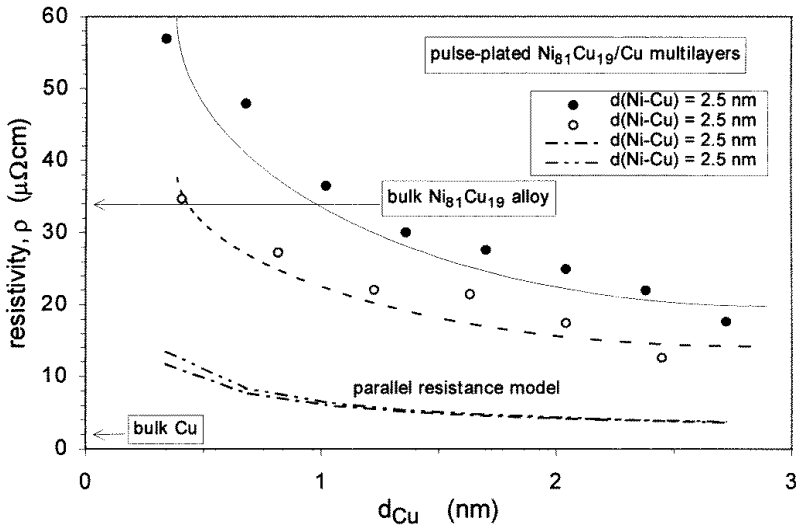

Figure 7. Room-temperature in-plane electrical resistivity (ρ) of electrodeposited $Ni_{81}Cu_{19}$/Cu multilayers with $d_{Ni-Cu} = 2.5$ nm (solid symbols and open symbols, denoting two different series) as a function of the Cu layer thickness (d_{Cu}). The solid and dashed lines through the data points serve as a guide for the eye only. The arrows to the ρ axis point to the resistivity of the bulk electrodeposited $Ni_{81}Cu_{19}$ alloy and to that of pure Cu. The results calculated on the basis of a parallel resistance model by using bulk resistivity values of Cu (2 $\mu\Omega$ cm) and $Ni_{81}Cu_{19}$ (34 $\mu\Omega$ cm) are given by the dash–dotted line for $d_{NiCu} = 2.5$ nm. The double-dot–dashed line gives the calculated resistivity in the above model for $d_{Ni-Cu} = 2.5$ nm by assuming that the magnetic layer has a composition of $Ni_{50}Cu_{50}$ exhibiting the maximum resistivity (60 $\mu\Omega$ cm) in the Ni–Cu system (see figure 3).

are given in figure 6 similarly as for ρ in figure 5. It can be seen that there is again a discrepancy between the thermopower values calculated as a crude approximation from equation (3) and the experimental data.

The room-temperature resistivity and thermopower were determined also for two series with constant magnetic layer thickness ($d_{Ni-Cu} = 2.5$ nm) as a function of the non-magnetic layer thickness d_{Cu} (figures 7 and 8, respectively). Although the ρ values are different for the two series, their variation with d_{Cu} still follows the same behaviour whereas the two sets of S data show a very good agreement. The decrease of ρ with increasing d_{Cu} (figure 7) corresponds to expectation although the parallel resistance model (dash–dot line) cannot again reproduce the experimental data, even with the assumption of a maximum-resistivity composition ($Ni_{50}Cu_{50}$) for the magnetic layers (double-dot–dash line in figure 7). For the thermopower, although the trend with increasing d_{Cu} is again correct, the volume average model still appreciably deviates from the experimental data (figure 8).

It is important to note that, as figures 5 and 7 demonstrate, for sufficiently thin Cu layers ($d_{Cu} < 1$ nm), the multilayer resistivity can definitely well exceed the resistivity of the bulk $Ni_{81}Cu_{19}$ alloy. This suggests that at such small layer thicknesses, the electrical resistivity may already contain a dominating contribution from surface scattering processes. Indeed, the results of previous studies [20, 21] have demonstrated such an increase of the resistivity of very thin metallic layers including Cu as well. Therefore, the large resistivity observed for the multilayer structure can probably be accounted for to a large extent by surface scattering processes occurring at the interfaces between the magnetic and non-magnetic constituent

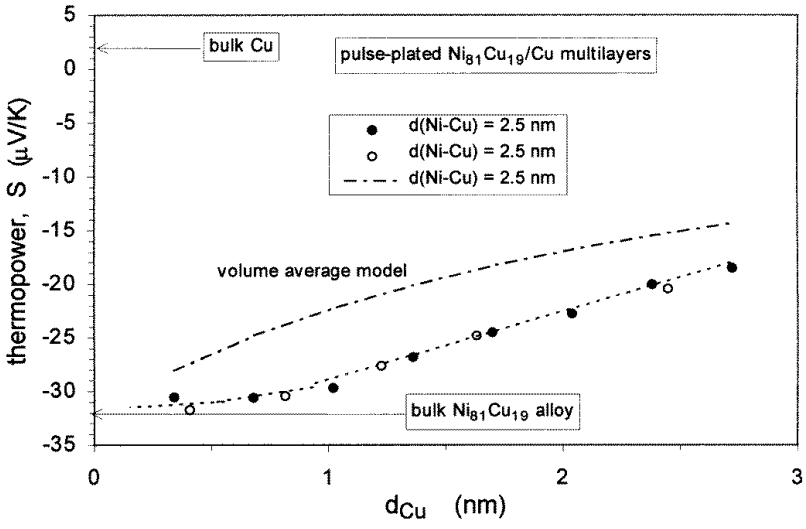

Figure 8. Room-temperature in-plane thermopower (S) of electrodeposited $Ni_{81}Cu_{19}$/Cu multilayers with $d_{Ni-Cu} = 2.5$ nm (solid symbols and light symbols, denoting two different series) as a function of the Cu layer thickness (d_{Cu}). The thin dashed line through the data points serves as a guide for the eye only. The arrows to the S axis point to the the thermopower of the bulk electrodeposited $Ni_{81}Cu_{19}$ alloy and to that of pure Cu. The results calculated on the basis of a volume average model by using bulk thermopower values of Cu (2.17 μV K^{-1}) and $Ni_{81}Cu_{19}$ (-32 μV K^{-1}) are given by the dash–dotted line for $d_{Ni-Cu} = 2.5$ nm.

layers. Such large resistivity values well exceeding the resistivities of any of the constituent bulk metals have actually been observed also for other nanoscale multilayers containing Cu such as Ni/Cu [22, 23], Ta/Cu [22] and Nb/Cu [24]. The actual resistivity enhancement beyond the bulk values can be influenced by surface (in multilayers: interface) roughness effects as well [22] that may be, e.g., an explanation for the difference in the magnitude of the resistivity values between the two multilayer series prepared under nominally identical conditions (see figure 7).

Although the importance of surface scattering processes in determining the thermopower of very thin layers has also been discussed in the literature [25], the situation is less clear for the Ni–Cu/Cu multilayers. As expected, $S(Ni_{81}Cu_{19}/Cu) \approx S(Ni_{81}Cu_{19})$ is obtained for large d_{Ni-Cu} and small d_{Cu} (figures 6 and 8). However, it is not easy to visualize the deviation of experimental S values from the 'volume average model' since even the qualitative interpretation of thermopower data is, in general, much more complicated than that of the resistivity. However, the fact that the thermopower data, in contrast to the resistivity, do not differ for the two series as a function of d_{Cu} (figure 8) indicates that the sensitivity of resistivity and thermopower to subtle structural details is not necessarily the same.

It should be mentioned that recent TEM studies [6] of these samples have revealed a significant inclination (up to 45°) of the multilayer planes with respect to the substrate plane at the top of the multilayer structure and this fact may also bear some significance with respect to the observed large resistivity. Since the measuring current flows in the foil plane parallel to the substrate plane (current-in-plane, CIP, configuration), in the top region of the multilayer the current actually flows at an angle to the multilayer planes (current-at-angle-to-plane, CAP, configuration). This means that the electrons should probably frequently pass the high-resistivity $Ni_{81}Cu_{19}$ layer as well. If d_{Cu} is not too high, the Cu layer will not be able,

due to the inclined multilayer planes, to effectively shunt the high-resistivity magnetic layers and we can expect that the multilayer resistivity will mainly be determined by the resistivity of the magnetic layer ($\rho_{CIP} \approx \rho_{Ni_{81}Cu_{19}}$). This effect might also be invoked when explaining the observation (figures 5 and 7) in that $\rho_{Ni-Cu/Cu} \approx \rho_{Ni_{81}Cu_{19}}$ (or $\rho_{Ni-Cu/Cu} > \rho_{Ni_{81}Cu_{19}}$) for sufficiently thin Cu layers. However, since the inclination of the multilayer planes [6] is restricted to the uppermost layers only and this feature occurs in a pronounced manner around $d_{Ni-Cu} \approx$ 2–3 nm only, it is still believed that the above described multilayer resistivity data are mainly influenced by surface scattering effects alone due to the nanometre-scale multilayer structure.

Although in discussing the resistivity data for electrodeposited bulk Ni–Cu alloys, the role of grain boundaries as a source of resistivity increase was also emphasized, this effect can be ruled out for the Ni–Cu/Cu multilayers since their TEM studies [6, 8] have revealed that they grow in a columnar form and the column width (i.e. the in-plane grain size) is typically several 100 nm.

4. Conclusions

The main objective of the present work was to investigate the room-temperature electrical transport properties (resistivity and thermopower) for electrodeposited nanoscale $Ni_{81}Cu_{19}$/Cu multilayers. The experimental data on several micrometre thick and substrate-free multilayer samples indicated a systematic variation of both parameters as a function of the magnetic ($Ni_{81}Cu_{19}$) and the non-magnetic (Cu) layer thickness.

Calculated resistivity values obtained in a parallel resistance model based on bulk resistivities of the sublayer materials remained significantly below the experimental data although they approached them with increasing sublayer thicknesses. We have argued that the main origin of the observed discrepancy lies in the nanoscale multilayer structure. Namely, it has been well documented in the literature that, in thin films of similar thicknesses as the sublayers in our multilayers, a significant surface scattering of electrons can greatly enhance the electrical resistivity beyond the bulk values and the same should happen also at the interfaces in the multilayer structure. The importance of these effects is exemplified by the fact that for multilayer series with a constant Cu thickness of about 1 nm, the experimental resistivity data exceeded the parallel resistance model by about a factor of two even for d_{Ni-Cu} as high as 10 nm (figure 5).

The experimental thermopower data were found to be more negative than by simply taking a volume average of the bulk values of the constituent sublayers. An increased surface scattering effect might be responsible also here for this difference. However, it is hard to make even a qualitative estimate at present to take into account the influence of surface scattering on thermopower of nanoscale multilayer films. On the other hand, the present study indicated a difference in sensitivity of the electrical resistivity and the thermopower to surface scattering processes as manifested also in the relatively good agreement of calculated and measured thermopower values (figure 6) for magnetic layer thicknesses where the parallel resistance model was still well below the experimental data.

References

[1] Ross C A 1994 *Annu. Rev. Mater. Sci.* **24** 159
[2] Schwarzacher W and Lashmore D S 1996 *IEEE Trans. Magn.* **32** 3133
[3] Lashmore D S, Zhang Y, Hua S, Dariel M P, Swartzendruber L and Salamanca-Riba L 1994 *Proc. 3rd Int. Symp.*

on Magnetic Materials, Processes, and Devices vol 94–6, ed L T Romankiw and D A Herman Jr (Pennington, NJ: Electrodeposition Division of the Electrochemical Society) p 205
[4] Bird K D and Schlesinger M 1995 *J. Electrochem. Soc.* **142** L65
[5] Bakonyi I, Tóth-Kádár E, Becsei T, Tóth J, Tarnóczi T, Cziráki Á, Geröcs I, Nabiyouni G and Schwarzacher W 1996 *J. Magn. Magn. Mater.* **156** 347
[6] Cziráki Á, Geröcs I, Fogarassy B, Arnold B, Reibold M, Wetzig K, Tóth-Kádár E and Bakonyi I 1997 *Z. Metallk.* **88** 781
[7] Tóth J, Kiss L F, Tóth-Kádár E,Dinia A, Pierron-Bohnes V and Bakonyi I 1999 *J. Magn. Magn. Mater.* at press
[8] Cziráki Á, Pierron-Bohnes V, Ulhaq-Bouillet C, Tóth-Kádár E and Bakonyi I 1998 *Thin Solid Films* **318** 239
[9] Tóth-Kádár E, Bakonyi I, Becsei T, Tóth J, Tarnóczi T, Pogány L, Kamasa P, Cziráki Á, Geröcs I, Nabiyouni G and Schwarzacher W 1999 to be published
[10] Bakonyi I, Tóth-Kádár E, Pogány L, Cziráki Á, Geröcs I, Varga-Josepovits K, Arnold B and Wetzig K 1996 *Surf. Coat. Technol.* **78** 124
[11] Tóth-Kádár E, Bakonyi I, Pogány L and Cziráki Á 1996 *Surf. Coat. Technol.* **88** 57
[12] Varga L, Tompa K and Schmidt T 1981 *Phys. Status Solidi* a **68** 603
[13] Tóth-Kádár E, Bakonyi I, Lóránth J, Sólyom A, Pogány L, Dankházi T, Tóth J, Konczos G, Fodor P and Liebermann H H 1990 *Plat. Surf. Finish.* **77** 70
[14] Ahern S A, Martin M J C and Sucksmith W 1958 *Proc. R. Soc.* A **248** 145
[15] Ahmad H M and Greig D 1974 *J. Physique Coll.* **35** C4 223
[16] Rodmacq B and dos Santos C A 1992 *J. Magn. Magn. Mater.* **109** 298
[17] *Landolt-Börnstein New Series* 1982 *Group III* vol 15a (Berlin: Springer)
[18] Roberts R B 1981 *Phil. Mag.* B **43** 1125
[19] Bakonyi I, Tóth-Kádár E, Tóth J, Cziráki Á and Fogarassy B 1994 *Nanophase Materials (NATO ASI Series E 260)* (Dordrecht: Kluwer) p 423
[20] Hoffmann H 1982 *Advances in Solid State Physics* vol 22 (Braunschweig: Vieweg) p 255
Vancea J 1989 *Int. J. Mod. Phys.* B **3** 1455
[21] Fenn M, Akuetey G and Donovan P E 1998 *J. Phys.: Condens. Matter* **10** 1707
[22] Reiss G, Kapfberger K, Meier G, Vancea J and Hoffmann H 1989 *J. Phys.: Condens. Matter* **1** 1275
[23] Sato H, Matsudai T, Abdul-Razzaq W, Fierz C and Schroeder P A 1994 *J. Phys.: Condens. Matter* **6** 6151
[24] Fenn M, Petford-Long A K and Donovan P E 1998 *3rd Int. Symp. on Metallic Multilayers (Vancouver, 1998)*
[25] Warkusz F 1980 *Progr. Surf. Sci.* **10** 287